Eur. Phys. J. A **12**, 185–190 (2001)

THE EUROPEAN PHYSICAL JOURNAL A

Nuclear temperatures obtained from light-charged-particle yields in low-energy ternary fission

M.N. Andronenko[1], L.N. Andronenko[1], W. Neubert[2,a], and D.M. Seliverstov[1]

[1] St. Petersburg Nuclear Physics Institute, Russian Academy of Science, 188300 Gatchina, Russia
[2] Institut für Kern- und Hadronenphysik, FZ Rossendorf, 01314 Dresden, Germany

Received: 10 August 2001 / Revised version: 1 October 2001
Communicated by D. Schwalm

Abstract. Nuclear temperatures were determined from yields of isotopes with $1 \leq Z \leq 14$ accompanying the spontaneous and neutron-induced fission of heavy elements. The mean temperature derived from the corresponding temperature distributions amounts to 1.10 ± 0.15 MeV.

PACS. 25.40.-h Nucleon-induced reactions – 25.85.-w Fission reactions

1 Introduction

The isotope thermometry which utilizes the double isotope-yield ratios [1] has been intensively studied in heavy-ion reactions. This approach provides results which are in agreement with other methods as far as the excitation energy of the emitting nuclei is restricted to $\simeq$ 3–5 AMeV [2,3]. Moreover, in ref. [4] it was demonstrated that the isotope thermometry gives also reasonable results in the case of proton-induced reactions p + Xe [5]. Although all isotopic pair combinations should give the same temperature, the extracted values fluctuate obviously from one to another choice of isotopes. Recently, we observed this behaviour in 1 GeV proton-nucleus reactions with various target nuclei from Be to U [6]. Otherwise, it was found that a fixed pair combination of isotopes delivers almost the same temperature, independent of the chosen target nucleus. But another isotope combination provided by the same target gives usually a different temperature. The reason of these fluctuations has been studied in several papers, *e.g.* [7,8]. Meanwhile, it is established that they arise from contributions of sequential decays of particle instable states in neighbour isotopes to the yield of a given isotope. A simple empirical method to correct for these fluctuations was proposed in [4]. As explained in the next section, the selection of isotopic pairs with differences (B) of their binding energies larger than 10 MeV minimizes the fluctuations considerably, but it decreases correspondingly the number of available isotope combinations. The temperatures derived from the remaining isotope combinations are assumed to be rather close to the intrinsic temperature of the emitting source. It was shown in ref. [6] that a selected double ratio of isotope yields delivers the same temperature for *various* projectile-target combinations. In dependence on the target mass, the corresponding temperatures show a similar stable behaviour like those selected with $B \geq 10$ MeV. This allows an application of such yield ratios for *relative* temperature measurements making a comparison between various projectile-target combinations.

If a sufficient large number of isotope thermometers is considered, one may expect that small fluctuations from sequential decays of different origin are partly canceled out. Therefore, we propose to use the whole ensemble of available isotope combinations to obtain Temperature Distribution (TD). Then the average of the distribution and its variance are supposed to be related to the intrinsic temperature and its dispersion, respectively. In the following, some selected data sets supply proof of these ideas and demonstrate the use of temperature distributions.

On the other side, one may ask for a class of fragment production reactions where distortions from sequential decays become a minimum. Such conditions should be realized if fragments are produced at very low excitation energies. Fission of heavy nuclei is a candidate of such a process. For the first time, we applied the isotope thermometry to yields of Ternary Charged Particles (TCP) accompanying the spontaneous and neutron-induced fission.

2 Application of isotope thermometry to ternary charged particles in fission

First we recall briefly the basic relations [1,4] to obtain the *apparent* isotopic temperature defined as

$$T_{\mathrm{app}} = \frac{B}{\ln(D_{\mathrm{s}} \cdot R)} \,. \qquad (1)$$

[a] e-mail: W.Neubert@fz-rossendorf.de

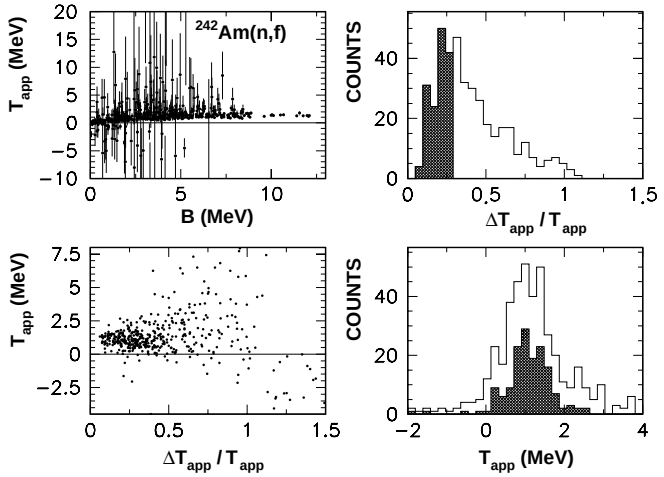

Fig. 1. Extraction of $T_{\rm app}$ distributions on the base of TCPs accompanying neutron-induced fission of ^{242}Am [20]. Left panels, top: $T_{\rm app}$ *versus* difference B of the binding energies, bottom: $T_{\rm app}$ *versus* the relative errors $\Delta T_{\rm app}/T_{\rm app}$. Right panels: projections onto the axes $\Delta T_{\rm app}/T_{\rm app}$ and $T_{\rm app}$. The shadowed part of the top histogram corresponds to the shadowed histogram of the bottom temperature distribution. Details are described in the text.

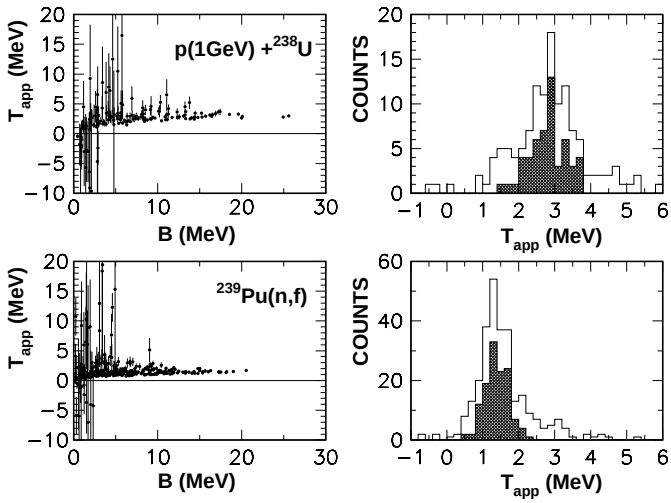

Fig. 2. Two-dimensional plots of temperatures $T_{\rm app}$ *versus* the difference B of the binding energies (left panels). Distributions of the isotope temperatures (right panels). Top: light isotopes from proton-uranium interactions [6]. Bottom: TCPs from neutron-induced fission of ^{239}Pu [16]. The solid histograms are obtained without cut in the relative error distribution. The influence of cuts is shown by the shadowed histograms: cut at $\Delta T_{\rm app}/T_{\rm app} \leq 0.17$ for p + ^{238}U, cut at $\Delta T_{\rm app}/T_{\rm app} \leq 0.13$ for ^{239}Pu(n, f).

The quantities in the denominator have the following meaning. $D_{\rm s}$ includes the spin degeneration factors and the mass numbers of the considered isotopes. $R = R_1/R_2$ is the double ratio and the single ratios R_1 and R_2 are given by the isotope yields (Y)

$$R_1 = Y(A_i, Z_i)\,/\,Y(A_i + \Delta A, Z_i + \Delta Z)\,,$$
$$R_2 = Y(A_j, Z_j)\,/\,Y(A_j + \Delta A, Z_j + \Delta Z)\,. \qquad (2)$$

Equation (1) assumes that the isotopes with mass A_i, A_j and nuclear charge Z_i, Z_j are produced in their ground states and sequential decay corrections to the yields are negligible. The numerator B is determined by the differences of the binding energies $E_{\rm b}$

$$B = E_{\rm b}(A_i, Z_i) - E_{\rm b}(A_i + \Delta A, Z_i + \Delta Z) - E_{\rm b}(A_j, Z_j) + E_{\rm b}(A_j + \Delta A, Z_j + \Delta Z). \qquad (3)$$

We term each combination of (R, $D_{\rm s}$, B) in eq. (1) a *thermometer* which allows to find the isotope temperature related to the fragment formation.

Here, the described method is exploited to extract temperatures from yields of TCPs which accompany the fission process. Most of the data are available for thermal-neutron–induced fission of heavy nuclei: ^{229}Th(n, f) [9], ^{233}U(n, f) [10,11], ^{235}U(n, f) [12–14], ^{239}Pu(n, f) [15,16], ^{241}Pu(n, f) [17], ^{242}Am(n, f) [16,18–20] and ^{245}Cm(n, f) [20,21]. Yields of TCP measured in the case of spontaneous fission of ^{252}Cf were taken from refs. [22–24]. The data listed above allow one to determine the temperatures using yields of isotopes within $1 \leq Z \leq 14$. We note that the meaning of TCP in the context of fission is related to ejectiles from hydrogen to silicon. The corresponding temperature is supposed to *remember* the stage of TCP emission during the fission dynamics.

Figure 1 shows by means of illustrative plots how we get a temperature distribution using the measured TCP yields for ^{242}Am(n, f) [20]. Just as in ref. [4] the temperatures are displayed as a function of the difference B of the binding energies. Every point on the scatter plot $T_{\rm app}$ *versus* B represents an individual thermometer. The error of $T_{\rm app}$ is calculated from the given experimental uncertainties of the isotope yields. One can see that some points are scattered away from the region where the bulk of thermometers is located. As a rule, such points have the largest errors (see also the following fig. 2). In fig. 1, this observation is sufficiently confirmed by the plot $T_{\rm app}$ *versus* $\Delta T_{\rm app}/T_{\rm app}$. In the following, values $T_{\rm app}$ with large relative errors can be removed by a simple cut set in the projection of the temperatures onto the axis $\Delta T_{\rm app}/T_{\rm app}$ (see fig. 1, right panels, top). After this selection, the temperature distribution represented by the shadowed histogram is generated (right panels, bottom). The mean value $\langle T_{\rm app}\rangle$ of this distribution was found to be insensitive to the chosen cut. Therefore, it is possible to apply the cut in the relative errors to remove unphysical negative temperatures (fig. 1, left panels, bottom).

In order to compare properly temperature distributions obtained for TCP accompanying low-energy fission with those for the fragmentation process we used the data related to isotope yields ($1 \leq Z \leq 5$) measured in proton-nucleus interactions at 1 GeV. A survey of available data is given in ref. [6]. Temperature distributions for the case of

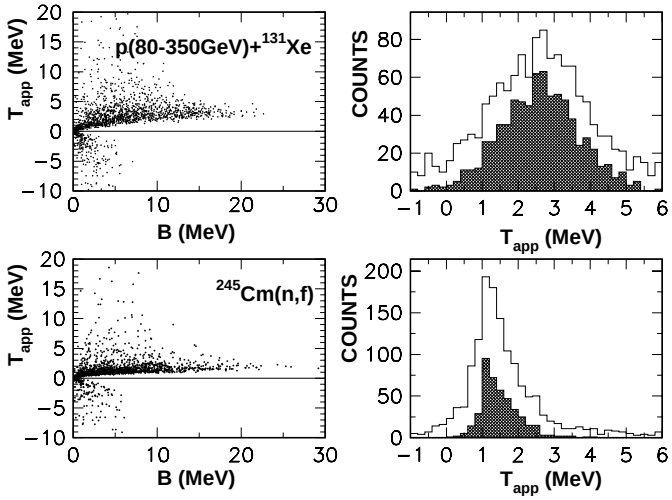

Fig. 3. The same as in fig. 2 for proton-induced reaction p + ^{131}Xe [5] (top panels); neutron-induced fission of ^{245}Cm [21] (bottom). Shadowed histograms: cut at $\Delta T_{\rm app}/T_{\rm app} \leq 0.10$.

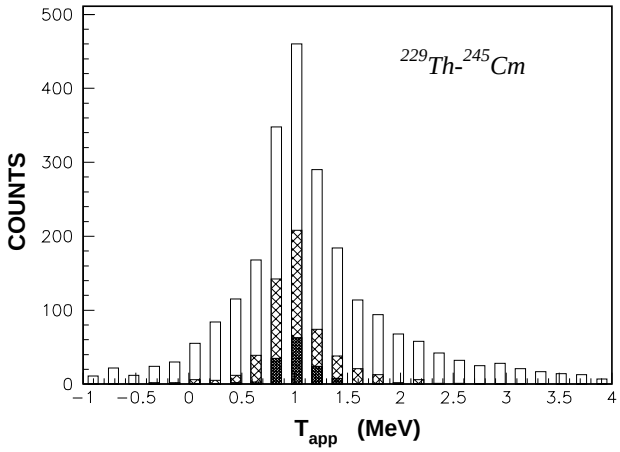

Fig. 4. Summary temperature distribution obtained from TCP in low-energy neutron-induced fission of heavy nuclei from ^{229}Th to ^{245}Cm. Only TCP with $Z \geq 3$ were selected (see text). Open bar histogram: no cut in $\Delta T_{\rm app}/T_{\rm app}$. Hatched histogram: cut at $\Delta T_{\rm app}/T_{\rm app} = 0.10$. Black histogram: cut at $\Delta T_{\rm app}/T_{\rm app} = 0.05$.

comparable target masses, namely 1 GeV proton-^{238}U collisions and thermal-neutron–induced fission of ^{239}Pu, are shown in fig. 2. The projections of the plots $T_{\rm app}$ *versus* B on the temperature axis are quite different for these two selected reactions. Beside the different mean values of the temperature distribution also the shape is much broader for the high-energy proton collisions compared with the corresponding one obtained from TCPs which accompany the fission of ^{239}Pu [16]. This behaviour is not trivial since a recent theoretical investigation of temperature distributions for the multifragmentation scenario [25] predicts that the variance σ_T^2 should be independent of the excitation energy. Here, we found that the extracted temperature distributions have different widths if the charged particles originate from fragmentation or from ternary fission. The reason of this difference cannot be the statistical errors of the isotope yields because they are similar in both data sets. This finding suggests that the widths of the temperature distributions are related to temperature fluctuations caused by completely different physical processes. We suggest that the higher average temperature and the larger variance of the temperature distribution in the case of 1 GeV p + U collisions is due to the production of excited isotopes from a hot source. On the other side, the corresponding fission temperatures which peak at an average of $T \simeq 1$ MeV hint to TCP production at low excitation energy. At the same time, a significant decrease of the fluctuations is observed.

We demonstrate the influence of the incidence energy on the temperature distribution by an additional example. Figure 3 shows a scatter plot of temperatures obtained from the isotopic yields in p + Xe collisions [5]. These data were obtained within the wide range of proton energies from 80 GeV to 350 GeV resulting in a broad temperature distribution. The exclusion of temperatures with large relative errors from this data set does not change this behaviour. Now we contrast this temperature distribution with the corresponding one obtained from yields of TCPs from the thermal-neutron–induced fission of ^{245}Cm [21]. The latter distribution is substantially narrower and peaks at $T \simeq 1.1$ MeV.

Whereas the dispersions of the temperature distributions obtained from fragmentation data vary with the energy of the incident proton beam, all analysed isotope thermometers of TCP accompanied fission deliver similar distributions centered at nearly the same mean value. This property gives us the opportunity to combine isotope temperatures $T_{\rm app}$ evaluated for target nuclei from ^{229}Th to ^{245}Cm into one temperature distribution characterized by $\langle T_{\rm app} \rangle = (1.10 \pm 0.15)$ MeV. We notice that this error results mainly from systematic uncertainties of the experimental data. Sufficient statistics allows to select isotope combinations with $Z \geq 3$ to avoid distortions of light-particle yields by decay modes like ^{5}He $\rightarrow$ ^{4}He + n and ^{7}He $\rightarrow$ ^{6}He + n, which cannot be distinguished from the intrinsic yields of the He isotopes. As shown in fig. 4 this selection leads to a slightly reduced average temperature of $\langle T_{\rm app} \rangle = 1.00$ MeV. In addition to the above given result for neutron-induced fission we present in fig. 5 the temperature distribution derived from TCPs associating the *spontaneous* fission of ^{252}Cf [24], but with the disadvantage of low statistics. Using the data on neutron decay of ternary particles in the spontaneous fission of ^{252}Cf [26] it becomes possible to correct the yields of He isotopes for contributions from the decay modes ^{5}He $\rightarrow$ ^{4}He + n and ^{7}He $\rightarrow$ ^{6}He + n. As a result, three times more thermometers can be considered. It is remarkably that both temperature distributions displayed in fig. 5 deliver the same averages of $\langle T_{\rm app} \rangle = (1.20 \pm 0.15)$ MeV. Although this temperature is slightly higher than the corresponding one for TCP accompanied fission, both results agree within the indicated

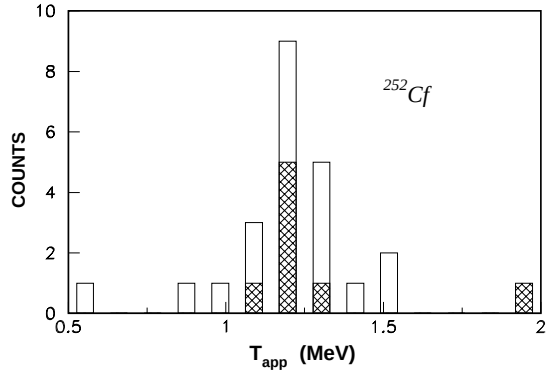

Fig. 5. Temperature distributions derived from TCP yields in the spontaneous fission of ^{252}Cf. Hatched bar histogram: data from ref. [24]. Open bar histogram: the same data corrected for the g.s. decay modes of ^{5}He and ^{7}He according to the measurements reported in ref. [26].

errors. The found temperature of 1.2 MeV is also consistent with the value of $T = (1.1 \pm 0.2)$ MeV [27] derived from the spectrum of neutrons accompanying the *ternary* fission of ^{252}Cf. In the *binary* mode of spontaneous fission of ^{252}Cf [28], a temperature of $T = (0.72 \pm 0.04)$ MeV was obtained from fits of the neutron spectrum with a Maxwell-Boltzmann distribution.

In comparison, the effective temperature estimated for 60 MeV ^{3}He induced fission of actinide elements was found to be $\langle T_{\rm eff} \rangle = (1.13 \pm 0.15)$ MeV [29]. We conclude from these agreements that the isotope thermometers provide reliable temperatures if they are extracted from the yields of TCPs accompanying fission.

It seems that the above-treated distributions of $T_{\rm app}$, derived from TCP in fission reactions, are very similar but a closer look shows that there is a small dependence on the mass of the fissioning system which will be discussed in the next section.

3 Target mass dependence of isotope temperatures in ternary fission and p + A fragmentation

More insight can be achieved by a detailed comparison of isotope temperatures evaluated for different reaction types, namely thermal-neutron–induced ternary fission and 1 GeV proton-induced fragmentation. For that purpose we analysed more than 10^3 thermometers, which are available for TCP accompanied fission, in dependence on the target mass $A_{\rm T}$. Data related to fragment production provided more than 10^2 thermometers. All extracted temperatures show a nearly linear dependence of $T_{\rm app}$ on $A_{\rm T}$ for the processes under consideration. We illustrate this feature in figs. 6 and 7 by some isotope thermometers which are identical for both classes of reactions. The choice of isotopic pairs with $\Delta A = 1$ and $\Delta Z = 0$ was made to minimize Coulomb effects upon the yields. However, this selection is of minor influence because the Coulomb correction is supposed to have no effect on the temperatures extracted from double isotope ratios [30]. The other presented combination of isotopic pairs with $\Delta A = \Delta Z = 1$ allows to remove the influence of the chemical potentials.

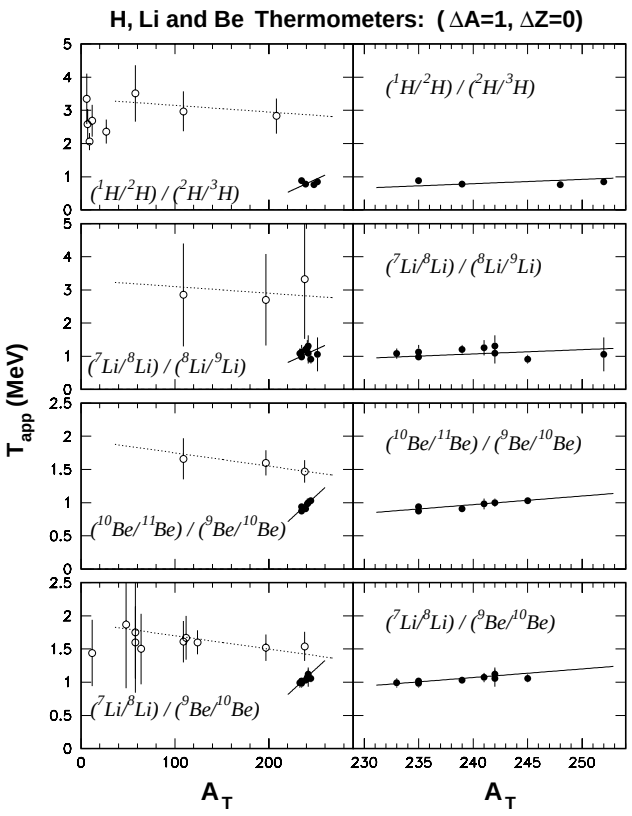

Fig. 6. Apparent temperatures as a function of the target mass $A_{\rm T}$. Selected combinations of isotopes with $\Delta A = 1$, $\Delta Z = 0$. Open circles in the left panels: p + A fragmentation, full circles: TCP accompanied fission. Right panels show the latter temperatures on an expanded mass scale. The solid lines in the right panels demonstrate the applicability of the obtained slope parameter c_2 to various isotope thermometers.

A first look on figs. 6 and 7 shows that the temperatures depend smoothly on the target mass for both classes of interactions. This behaviour is expected in an equilibrated system if the excitation energy changes weakly with the mass. But the temperatures $T_{\rm app}$ differ considerably in the two interaction mechanisms with regard to the absolute value (see also fig. 2). A further difference in the two data sets becomes apparent if the obtained temperatures $T_{\rm app}$ are fitted by a linear dependence on $A_{\rm T}$. We excluded fragmentation data of the lightest nuclei from the fit procedure so that only targets with $Z_{\rm T} \geq 28$ (Ni) were taken into account. The slight decrease of $T_{\rm app}$ obtained for p + A fragmentation can be quantified by

$$T_{\rm app} = c_1 + c_2 \cdot A_{\rm T}\,, \qquad (4)$$

where the average value of the parameter c_2 amounts to

$$c_2 = -(0.0020 \pm 0.0005)\ \ {\rm MeV}\,.$$

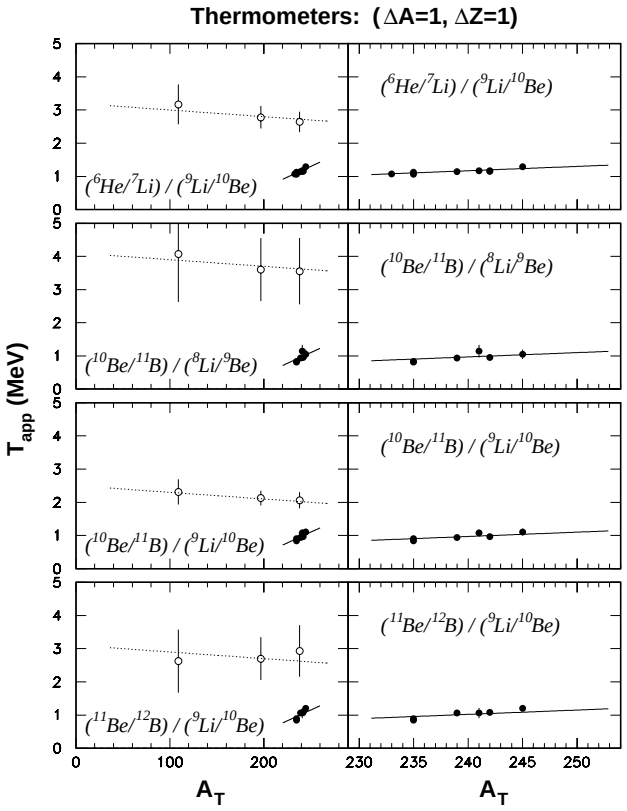

Fig. 7. Apparent temperatures *versus* target mass $A_{\rm T}$ selected by $\Delta A = 1$, $\Delta Z = 1$. The notations are the same as in fig. 6.

Just this common slope c_2 is displayed in figs. 6 and 7 by dotted lines for all thermometers related to fragmentation induced by 1 GeV protons.

If we interpret $T_{\rm app}$ as the temperature where the nuclei become stable against particle decay then the equivalent thermal excitation energy E^* corresponds to the separation energy of one nucleon. Otherwise, the chemical potential μ is the energy change when one particle is removed. Assuming i) that μ is nearly constant over the periodic table $\mu \simeq 8$ MeV and ii) that the level density parameter a can be approximated by $a \simeq A_{\rm T}/8\,{\rm MeV}$, then the Fermi gas relation reads

$$T = \sqrt{\frac{E^*}{a}} = \sqrt{\frac{\mu}{a}} \simeq \frac{8\,{\rm MeV}}{\sqrt{A_{\rm T}}}. \qquad (5)$$

From relation (3) we find for $50 \leq A_{\rm T} \leq 250$ a slope of $\Delta T/\Delta A_{\rm T} \simeq -3 \cdot 10^{-3}$ MeV which is close to the above value of c_2. Concerning low-energy ternary fission, the *opposite* mass dependence was found for the corresponding data set (see solid lines in figs. 6 and 7):

$$c_2 = +(0.013 \pm 0.004)\ \ {\rm MeV}\,.$$

The slope parameter in this case is about one order of magnitude larger compared with that obtained from p + A fragmentation. The thermal excitation energy of the excited residual nuclei dominates over the Coulomb part in the fragmentation process. The decrease of the temperature with $A_{\rm T}$ is qualitatively described by relation (5). Otherwise, only a part of the fissioning system seems to be involved into the TCP emission. The positive slope in this case reflects perhaps the increasing yield ratio of ternary to binary fission products with increasing fissility parameter Z^2/A. Furthermore, we found that the values $T_{\rm app}$ extracted from TCP yields have very small deviations with respect to the fit line. This finding suggests that these temperatures reflect a narrow distribution of the corresponding excitation energy of the emitting source and that contributions from sequential decays to the TCP yields are reduced in comparison to the fragmentation.

4 Summary and conclusions

Nuclear temperatures were evaluated from double yield ratios of light isotopes associated with spontaneous fission of ^{252}Cf *and* neutron-induced fission of heavy nuclei from ^{229}Th to ^{245}Cm. The applied method [1] is based on the general assumption that thermal equilibrium is achieved. This condition may be not fulfilled in the case of TCP production usually described by the emission during the non-adiabatic neck rupture. Nevertheless, the application of the thermal approach delivered results which agree surprisingly with temperatures established by other methods. Temperature distributions including most of the measured isotopic yields have been used to analyse the data instead of a formerly used selection criterion based on the difference B of the binding energies. All considered distributions of $T_{\rm app}$ are in agreement with $\langle T_{\rm app} \rangle = (1.10 \pm 0.15)$ MeV. The same isotope combinations available for 1 GeV proton-induced fragmentation deliver larger temperatures. We demonstrated by corresponding cross-checks that the isotope thermometry, mainly exploited in heavy-ions physics, can be extended also to ternary charged-particle production in low-energy fission of heavy nuclei. The dependence of $T_{\rm app}$ on the target mass $A_{\rm T}$ was investigated. The sign of the slope $T_{\rm app}$ *versus* $A_{\rm T}$ was found to be opposite in the two considered processes, *i.e.* TPC emission in low-energy fission and light-charged-particle production in proton-induced fragmentation. In conclusion one may speculate to use the extracted temperatures in the caloric curve of nuclear matter [31,32]. A measure of the intrinsic excitation energy near the scission point where TCP emission occurs should be the energy dissipated in the descent from the saddle to the scission of fissioning nuclei. The experimental values, extracted from the odd-even effect in the fragment charge distributions of binary fission, are rather small. In this particular case, energies within 3 MeV (Th) and 11 MeV (Cf) have been found [33]. Thereby, one has the opportunity to indicate the trend of the caloric curve to very low thermal excitation energy per nucleon.

This work was supported by the German Ministry of Education and Research (BMBF) under contract RUS-622-96 and by the Russian Foundation for Fundamental Research Grant No. 95-02-03671.

References

1. S. Albergo et al., Nuovo Cimento **89**, 1 (1985).
2. M. Milazzo et al., Phys. Rev. C **58**, 953 (1998).
3. O. Lopez et al., Nucl. Phys. A **685**, 246c (2001).
4. M.B. Tsang et al., Phys. Rev. Lett. **78**, 3836 (1997).
5. A.S. Hirsch et al., Phys. Rev. C **29**, 508 (1984).
6. M.N. Andronenko et al., Eur. Phys. J. A **8**, 9 (2000).
7. H. Xi et al., Phys. Rev. C **59**, 1567 (1999).
8. A. Kolomiets et al., Phys. Rev. C **54**, R472 (1996).
9. M. Wöstheinrich, Ph.D. thesis, Eberhard-Karls-Universität Tübingen, 1999.
10. A.A. Vorobyov et al., Phys. Lett. B **30**, 332 (1969).
11. M. Wöstheinrich et al., in *Proceedings of the 2nd International Workshop on Nuclear Fission and Fission-Product Spectroscopy, Seyssins, France, 1998*, edited by G. Fioni et al., AIP Conf. Proc. **447**, 330 (1998).
12. M. Dakowski et al., Phys. Lett. B **25**, 213 (1967).
13. A.A. Vorobyov et al., Phys. Lett. B **40**, 102 (1972).
14. W. Baum, Ph.D. thesis, TH Darmstadt, 1992.
15. T. Krogulski et al., Nucl. Phys. A **128**, 219 (1969).
16. A.A. Vorobyov et al., Sov. J. Nucl. Phys. **20**, 248 (1975).
17. U. Köster et al., Nucl. Phys. A **652**, 371 (1999).
18. U. Nast-Linke, Diplomarbeit, TH Darmstadt, 1992.
19. S. Neumaier, Diplomarbeit, TH Darmstadt, 1992.
20. M. Hesse, Ph.D. thesis, Eberhard-Karls-Universität, Tübingen, 1997.
21. U. Köster, Ph.D. thesis, TU München, 2000.
22. S.V. Cosper et al., Phys. Rev. **154**, 1193 (1967).
23. J.F. Wild et al., Phys. Rev. C **32**, 488 (1985).
24. Z. Dlouhy et al., HMI -B **464**, 43 (1989) unpublished; in *Nuclei Far From Stability and Atomic Masses and Fundamental Constants 1992: Proceedings of the 6th International Conference on Nuclei Far From Stability and the 9th International Conference on Atomic Masses and Fundamental Constants, Mainz, Germany, 19-24 July 1992*, edited by R. Neugart, A. Wöhr, *Inst. Phys. Conf. Ser.*, Vol. **132** (IOP, Bristol, 1993) p. 481.
25. S.R. Souza et al., Phys. Rev. C **62** 064607 (2000).
26. M. Mutterer, in *Seminar on Fission, Pont d'Oye IV*, edited by C. Wagemans, O. Serot, P. D'hondt (World Scientific, Singapore, 2000) p. 95.
27. A.P. Graevsky et al., Pis'ma Zh. Eksp. Teor. Fiz. **15**, 572 (1972).
28. H.R. Bowman et al., Phys. Rev. **126**, 2120 (1962).
29. S.D. Beisin et al., Yad. Fiz. **50**, 320 (1989).
30. J. Tõke et al., Phys. Rev. C **63**, 024606 (2001).
31. J. Pochodzalla et al., Phys. Rev. Lett. **75**, 1040 (1995).
32. S.J. Lee, A.Z. Mekjian, Phys. Rev. C **56**, 2621 (1997).
33. F. Gönnenwein, in *The Nuclear Fission Process*, edited by C. Wagemans (CRC Press, Boca Raton-Ann Arbor-Boston-London, 1991).